Improved mechanical dispersion or use of coupling agents? Advantages and disadvantages for the properties of fluoropolymer/ceramic composites

(Article begins on next page)

03 May 2024

**Improved mechanical dispersion or use of coupling agents? Advantages and disadvantages for the properties of fluoropolymer/ceramic composites**

Sara Dalle Vacche[a,1*], Véronique Michaud[a,2], Dragan Damjanovic[b], Jan-Anders E. Månson[a,3] Yves Leterrier[a,2*]

[a] Laboratoire de Technologie des Composites et Polymères (LTC), Ecole Polytechnique Fédérale de Lausanne, EPFL-STI-IMX-LTC, Station 12, CH-1015 Lausanne, Switzerland

[b] Group for Ferroelectrics and Functional Oxides, Ecole Polytechnique Fédérale de Lausanne, EPFL-SCI-STI-DD, Station 12, CH-1015 Lausanne, Switzerland

e-mail addresses: sara.dallevacche@polito.it, veronique.michaud@epfl.ch, dragan.damjanovic@epfl.ch, jmansson@purdue.edu, yves.leterrier@epfl.ch

* Corresponding authors:

Yves Leterrier, EPFL-STI-IMX-LPAC, Station 12, CH-1015 Lausanne, Switzerland.

Phone: +41213964848 Fax: +41216935880 e-mail: yves.leterrier@epfl.ch

Sara Dalle Vacche, Department of Applied Science and Technology, Politecnico di Torino, C.so Duca degli Abruzzi 24, 10129 Torino, Italy.

Phone: +390110904630 e-mail: sara.dallevacche@polito.it

---

[1] Present address: Department of Applied Science and Technology, Politecnico di Torino, C.so Duca degli Abruzzi 24, 10129 Torino, Italy

[2] Present address: Laboratory for Processing of Advanced Composites (LPAC), Ecole Polytechnique Fédérale de Lausanne, CH-1015 Lausanne, Switzerland

[3] Present address:  Composites Manufacturing & Simulation Center, Purdue University, West Lafayette, IN 47906, USA

**Abstract**

The aim of this work is to investigate the influence of interfacial chemistry on the properties of fluoropolymer composites, independent of effects derived from changes in morphology, in particular particle dispersion state. A comparative study of solvent cast composites of poly(vinylidene fluoride – trifluoroethylene) with barium titanate particles, at concentrations up to 60 vol%, was carried out using pristine hydrophilic particles, and particles hydrophobized with three organosilanes, bearing different functional groups ($-CH_3$, $-CH_2NH_2$ and $-CF_3$). For each filler concentration, composites with good particle dispersion and comparable amount of porosity with all types of particles were prepared and characterized. While pristine particles provided higher permittivity, all silanes decreased the dielectric losses due to Maxwell-Wagner-Sillars dispersion, although to different extents. Moreover, only the aminosilane provided better thermomechanical stability to the highly filled composites. These results provide useful insights into the advantages and disadvantages of the use of different approaches to improve the dispersion of hydrophilic particles in poly(vinylidene fluoride) copolymer based composites.

1. **Introduction**

Dielectric composites exploit the high permittivity of some lead-free perovskite ceramics, as well as the flexibility, ease of processing and high dielectric breakdown strength inherent to polymers.  These have attracted great attention as materials for embedded or high energy density capacitors, for e.g. for electronics and energy storage. Among the materials most

2

frequently used as matrix in dielectric composites are the polymers based on poly(vinylidene fluoride) (PVDF). PVDF can crystallize in five polymorphs, α, β, γ, δ, and ε, having different chain conformations. While PVDF homopolymer crystallizes spontaneously in the *trans-gauche-trans-gauche'* (TGTG') α-phase, the phase showing the higher dielectric constant is the *all-trans* (TTTT) β-phase, in which all dipoles are aligned in the same direction. The introduction of trifluoroethylene moieties, such as in poly(vinylidene fluoride – trifluoroethylene), i.e. P(VDF-TrFE) investigated in the present work, favors spontaneous crystallization in a ferroelectric phase similar to the β-phase of PVDF. An increase in the amount of β-phase in PVDF and PVDF copolymers, e.g., by stretching, crystallization from appropriate solvents, or annealing, enhances the relative permittivity $\varepsilon_r$, but only to a certain limit, reaching values of up to 15 at room temperature [1,2]. Ceramics, such as barium titanate, $BaTiO_3$, or barium strontium titanate, $Ba_xSr_{(1-x)}TiO_3$, have relative permittivity of the order of thousands [3,4]. If they can be incorporated into polymers, at high volume fractions without compromising the mechanical properties, dielectric losses and breakdown strength, these fillers lead to the formation of composites with high permittivity. However, above a certain volume fraction, namely between 0.3 and 0.5 depending on the processing conditions, composites made with pristine ceramic particles are typically reported to suffer from overall property degradation. This is due primarily to the high contrast between the surface energy of the hydrophilic oxides and that of the hydrophobic fluorinated polymer, which leads to agglomeration and poor dispersion of the particles, formation of voids and interfacial defects [5–7]. Hot pressing proved to be a convenient route for obtaining PVDF-based composites with low porosity up to high filler concentrations, without necessarily improving particle dispersion, but this was at the expense of polymer crystallinity, and of the amount of β-phase, which were reduced with respect to solvent casting [6,8,9].

In order to produce highly filled composites with good dispersion and low porosity, a widely used approach is to use coupling agents. These include silanes, phosphonic acids, or other surface modification methods that reduce the surface energy contrast between ceramic fillers and polymers, and in general favor filler dispersion and overall improve the properties of the

composite [10–12]. For instance, BaTiO$_3$ particles or nanofibers, surface treated with sodium dodecyl sulfate, fluorosilanes or aminosilane, produced well dispersed PVDF composites, showing improved β-phase fraction, transparency, and dielectric properties, whereas the corresponding pristine fillers remained agglomerated and led to higher porosity and worse properties [13–17]. In these works, however, the very different dispersion states may have partly or entirely concealed effects purely due to interfacial chemistry.

Interestingly, well-dispersed composites have recently been obtained with pristine particles, by using mixing processes that rely on high mechanical energy to break the particle aggregates, e.g. ball milling and solid-state dispersion. These composites were compared to composites with surface modified particles having a similar morphology, obtaining inconsistent results for the contribution of coupling agents to the composite properties. For instance, polypropylene/nanosilica composites showed worse mechanical and thermal degradation properties when particles were modified with hexamethyldisiloxane, compared to pristine particles [18]. On the other hand, PVDF composites showed better matrix-filler adhesion, due to electrostatic interactions, and showed enhanced breakdown strength when fluorocarboxylic acid coated BaTiO$_3$ particles were used versus pristine particles, because the modifier formed a transition layer, blocking charge carriers, while permittivity was diminished [19]. In these works, however, only one type of coupling agent was used, and it is therefore not possible to know whether a different interfacial chemistry would have led to different results. Only few studies compared BaTiO$_3$ filled composites, all having similar morphology, in which particles were pristine or modified with a number of different coupling agents. Such studies were reported e.g. for epoxy- and HDPE- based composites, which properties differed depending on interfacial interactions. These differences were attributed, first, to different interactions of the chemical groups of the ligands with the polymer chains, including reaction with the thermoset polymer or electrostatic interactions; and second, for the HDPE composites, to different entanglement levels of the chains of the coupling agents with the polymer chains [20,21]. Indeed, the results above give clear indications that the effects of interfacial chemistry must be more deeply

understood to make better informed choices about the overall strategies for improving filler dispersion.

Contributing to this effort, we performed a comparative work focusing on PVDF copolymer composites. In order to simplify the identification of interfacial chemistry effects, we selected for the surface modification of $BaTiO_3$ three organosilanes that differed only for the functional group at the end of the organic chain ($-CH_3$, $-CH_2NH_2$ or $-CF_3$). Building on our previous results [6,17], we focused on the thermomechanical properties up to 150° C and on the dielectric properties at room temperature. We obtained dynamic mechanical analysis and dielectric spectroscopy data for solvent cast P(VDF-TrFE)/$BaTiO_3$ composites with pristine particles having good filler dispersion and low porosity for particle volume fractions as high as 0.6, which were, to the best of our knowledge, not previously available. We then compared these results to the ones obtained with silylated particles, relating the observed differences to the different surface chemistry of the fillers.

## 2. Materials and methods

### 2.1. Materials

P(VDF-TrFE) with 77 mol% VDF and 23 mol% TrFE, was provided in powder form by Solvay Solexis SpA (Italy). $BaTiO_3$, 99.95%, electronic grade, average particle size 0.2 µm, was purchased from Inframat Advanced Materials LLC, USA. The silane coupling agents, (3-aminopropyl)triethoxysilane, 99%, (3,3,3-trifluoropropyl)trimethoxysilane, 97% and *n*-propyltrimethoxysilane, 97%, were supplied by Sigma-Aldrich (USA), and in what follows they will be named APTES, TFTPMS and PTMS, respectively. Their structures are shown in Fig. 1. Methyl ethyl ketone, MEK, 99+ %, and ethanol, 99.5%, were supplied by Acros Organics (Belgium).
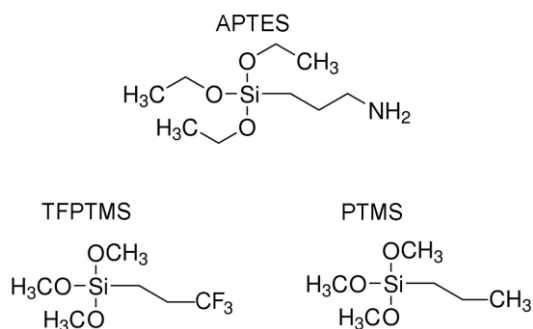
**Fig. 1.** Structures of the silanes used in this work: (3-aminopropyl)triethoxysilane (APTES), (3,3,3-trifluoropropyl)trimethoxysilane (TFPTMS), and *n*-propyltrimethoxysilane (PTMS).

*2.2. Surface modification of BaTiO$_3$*

BaTiO$_3$ was modified in an ethanol/water (95/5 v/v) solution with the following procedure. BaTiO$_3$ was first dispersed in ethanol, at a concentration of 0.4 g/ml, with an Ultra-Turrax T25 digital disperser (IKA Werke GmbH & Co. KG, Germany) for 15 min at 10000 rpm. Then the mixture was sonicated with a Sonifier 450 digital ultrasonic horn (Branson Ultrasonics Corporation, USA) at 40% intensity, with 5 s on / 5 s off pulses, applying ultrasounds for an effective time of 5 min. Finally, the deionized water and the desired silane were added, and the solution was stirred for 2.5 h at 70 °C. After centrifugation at 8000 rpm for 10 min (Heraeus Biofuge Primo Centrifuge, Thermo Fisher Scientific Inc., USA) the precipitated powder was dried at 110° C for 30 min to promote silanol condensation, ground in a mortar, washed twice with ethanol, dried again in a vacuum oven overnight, then kept in a desiccator until further use. Trifunctional silanes can attach with one, two, or three of their hydrolysable groups to the hydroxyl groups present on the surface of the particles [22]. To calculate the minimum amount of silane needed to ensure a complete monolayer coverage of the BaTiO$_3$ particles it was assumed that the concentration of hydroxyl groups on the surface of the BaTiO$_3$ particles, available for reaction with the silanes was 13.8 OH/nm$^2$ [23] , and that each silane molecule reacted with only one surface hydroxyl group. Under these assumptions, 0.026 g of APTES or TFPTMS or 0.019 g of PTMS per gram of BaTiO$_3$ would be necessary for complete consumption of the surface hydroxyl groups. Therefore, a slight excess of silane, i.e. 0.03 g

silane per gram of BaTiO$_3$, was used in the surface modification. In what follows, BT will indicate pristine BaTiO$_3$ particles, and BT-A, BT-F, and BT-P will indicate particles modified by APTES, TFPTMS and PTMS, respectively.

*2.3. Fabrication of solvent cast films*

The procedure used for the fabrication of the composite films was based on that used in previous work [17], however the concentration of polymer with respect to the solvent was increased to prevent settling of the particles, the sample was homogenized at higher speed to improve particle dispersion, and the thickness of the films was reduced to allow more homogeneous evaporation of the solvent. According to this updated procedure, a solution was prepared dissolving P(VDF-TrFE) at a concentration of 10 wt% in MEK at 60 °C. For the composites, appropriate quantities of of BaTiO$_3$, pristine or silylated, were slowly added to the P(VDF-TrFE)/MEK solution while stirring in order to obtain materials with particle volume fractions $\phi$ equal to 0.15, 0.3, 0.45 and 0.6. The density of BaTiO$_3$ was taken equal to 5.8 g cm$^{-3}$ according to the supplier's information, and that of P(VDF-TrFE) equal to 1.9 g cm$^{-3}$ [24]. The mixtures were stirred with a magnetic stirrer for 1 h at 60 °C, sonicated with the Sonifier 450 with 5 s on/ 5 s off pulses for a total ultrasound time of 5 min, and homogenized with the Ultra-Turrax T25 at 10000 rpm for 15 min.  After degassing in vacuum, the mixtures were cast on glass and dried in a vacuum oven at 80 °C for 4 h. The films, 40-50 µm thick, were detached from the glass support and annealed at 135 °C for 30 min to increase crystallinity.

*2.4. Characterization techniques*

Thermogravimetric analysis (TGA) was used to verify the surface modification of the BaTiO$_3$ particles. It was performed with a TGA/SDTA 851 apparatus (Mettler Toledo, Switzerland), heating from 30 °C to 800 °C at 10 °C min$^{-1}$ under N$_2$ flow (30 ml min$^{-1}$).

Freeze fractured surfaces of the nanocomposites were carbon coated to prevent charging and observed with a XL30 FEG (Philips, The Netherlands) scanning electron microscope (SEM).

The density of the nanocomposites with $\phi$ = 0.45 and 0.6 was determined by Archimede's principle, with an AT261 DeltaRange balance equipped with a density kit ME-210250 (Mettler Toledo, Switzerland). The porosity was then estimated for each composite by comparing the measured density to the theoretical one calculated on the basis of the mass fractions and densities of the matrix and filler.

The crystal structures of P(VDF-TrFE) and of $BaTiO_3$ were probed by X-ray diffraction (XRD) on a D8 Discover diffractometer (Brucker AXS, USA) with CuKα radiation.

Differential scanning calorimetry (DSC) was used to determine the phase transition temperatures and the degree of crystallinity of P(VDF-TrFE), alone and in the composites. The measurements were carried out heating at 10 °C $min^{-1}$ from 0 °C to 180 °C and then cooling from 180 °C to 0 °C at 10 °C $min^{-1}$.

The thermomechanical properties were measured by dynamic mechanical analysis (DMA) in tensile configuration with a Q800 DMA (TA Instruments, USA). The measurements were performed on 6 mm wide rectangular specimens, between -80 °C and 150 °C, at a heating rate of 3 °C $min^{-1}$ and a frequency of 1 Hz. The strain was fixed at 0.05 % in order to stay within the linear viscoelastic range of the materials.

For the dielectric characterization gold electrodes were deposited on both sides of the films by sputtering, and square specimens with an area of about 40 $mm^2$ were then cut. Capacitance and loss tangent were measured at room temperature as a function of frequency with an Agilent 4294A Precision Impedance Analyzer (Agilent Technologies, Inc., USA) between $10^2$ and $10^7$ Hz, with a voltage of 0.5 $V_{rms}$. Relative permittivity was then calculated from capacitance, knowing the electrode-covered area and the thickness of each sample.

## 3. Results and discussion

### 3.1. Surface modification of the particles

The surface modification of the $BaTiO_3$ particles was verified by TGA (Fig. 2). In the temperature interval up to 300 °C, while the silylated powders showed a weight loss of less than 0.1 wt%, the pristine $BaTiO_3$ powder lost 0.15 wt%. This weight loss was mainly ascribed to adsorbed water, released below 200 °C; the difference may therefore indicate that less water was adsorbed on silylated powders, due to their lower hydrophilicity. The pristine $BaTiO_3$ showed a second weight loss, above 450 °C, of an additional 0.18 wt%, attributed to the loss of surface hydroxyls. This loss matches reasonably well with the theoretical surface hydroxyl content calculated taking a surface concentration of 13.8 OH groups per $nm^2$, as indicated above, which corresponds, for 200 nm particles, to $1.2 \times 10^{-4}$ mol OH per gram of $BaTiO_3$, i.e 0.20 % in weight. For the silylated powders the second weight loss already started at 300 °C. BT-A and BT-P showed gradual weight loss until 800 °C, of additional 0.35 wt% and 0.3 wt%, respectively, while BT-F showed a steeper weight loss of additional 0.35 wt%, up to 650 °C, with no further change up to 800 °C. This may be attributed to a lower thermal stability of the fluorosilane, due to the presence of an electron withdrawing group [25]. For the silylated powders the weight loss above 300 °C can be related to the loss of the grafted silane chains. The theoretical weight loss calculated in the hypothesis that each OH group was replaced by one silane molecule would be of 0.6 wt%, 1.15 wt% and 0.51 wt% for BT-A, BT-F and BT-P respectively. Therefore, the TGA data implied that only slightly more than half of the theoretical maximum amount of silane was grafted for BT-A and BT-P, and only about one third for BT-F, although a slight excess of silane was used during the powder modification. This may indicate either a low efficiency of the silylation reaction, or that each silane molecule was attached with more than one hydrolysable group to the particle surface.
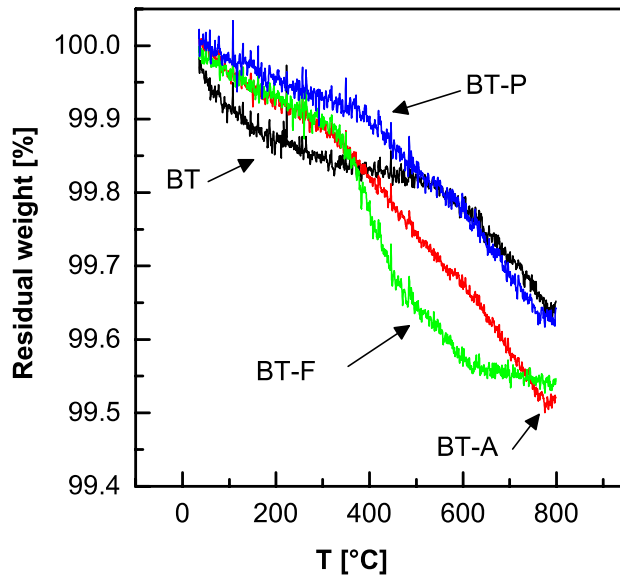
**Fig. 2.** Thermogravimetric analysis of the pristine and surface treated BaTiO$_3$ particles.

*3.2. Morphology and structure of the composites*

The SEM observation of the freeze-fractured surfaces of the composite films (Fig. 3) showed in all cases a homogeneous through thickness distribution of the filler and particle dispersion was overall good, with only few small aggregates still present. The matrix infiltrated well in the spaces between the BaTiO$_3$ particles. Upon fracture, the BT and BT-A particles remained well covered by the matrix. In the case of BT-F and BT-P, particles with matrix free surface could be observed, indicating weak matrix-filler adhesion. The SEM observation did not highlight large voids, while small pores with dimensions ranging from less than 100 nm to approximately 1 μm were visible. The density measurements of the composites with $\phi$ = 0.6 indicated about 16 % porosity with BT particles, 11 % porosity with BT-A particles, and 9% porosity with BT-F and BT-P particles. For all composites with $\phi$ = 0.45 the measured density matched the theoretical one, indicating that porosity was negligible. In our previous work, where less intense mixing conditions were used, the porosity with $\phi$ = 0.6 of pristine BaTiO$_3$ particles was about 28%, and large aggregates were present, while with the same volume fraction of APTES treated particles porosity was reduced to about 18% and particle dispersion was improved [17].
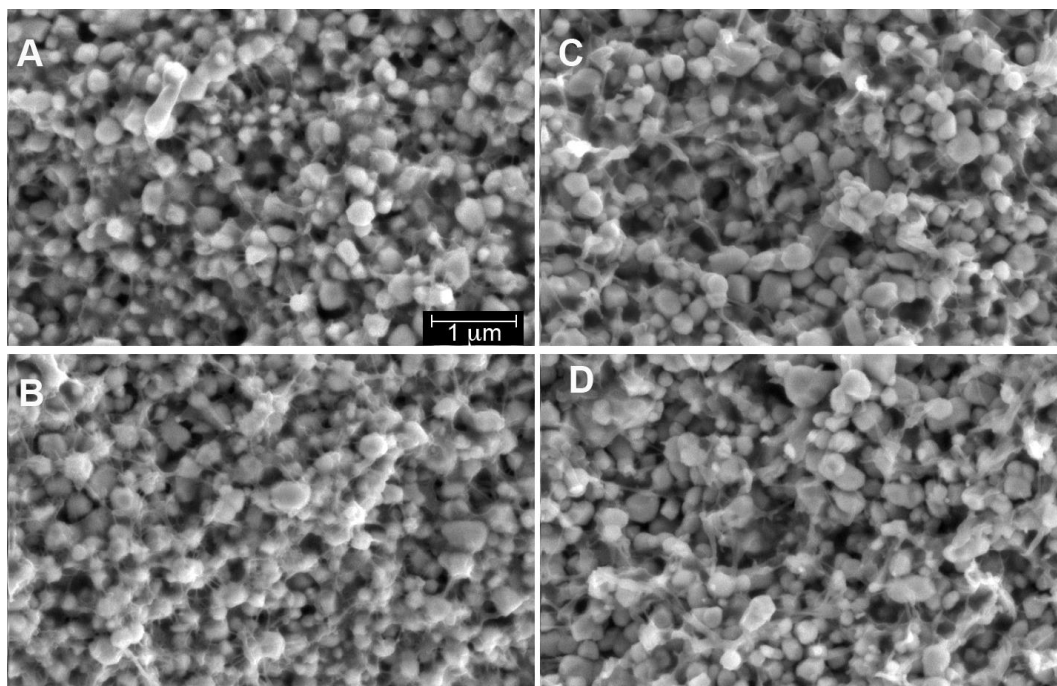
10

**Fig. 3.** SEM images of freeze fractured surfaces of composite films ($\phi$ = 0.6) containing: (A) BT, (B) BT-A, (C) BT-F and (D) BT-P

The heating and cooling DSC scans (Fig. 4) showed substantially similar patterns for the composites made with pristine and modified particles. The Curie transition peak during the cooling cycle appears at lower temperature than in the heating cycle, showing the thermal hysteresis behavior typical of PVDF copolymers similar to that used in this work, related to the first-order character of the ferroelectric-to paraelectric phase transition, as documented in literature [26–28]. Some small differences in the shape and position of the peaks, which did not seem to be correlated with the type of surface modification of the particles, appeared mostly for the highly filled films, and are thought to be likely related to process variability. The cooling and heating scans for composites with $\phi$ = 0.15 and $\phi$ = 0.6 are given in Fig. 4; the scans for composites with $\phi$ = 0.3 and $\phi$ = 0.45 were very similar to those obtained for $\phi$ = 0.15 and are reported in Supplementary Information (Figure S1). The melting and crystallization enthalpies (Fig. 5) scaled with the volume fraction of BaTiO$_3$ in good agreement with the theoretical calculation until $\phi$ = 0.45, indicating negligible effect of the particles on the crystallinity of the matrix. A very slight decrease of the measured enthalpies with respect to the theoretical ones,

and hence of crystallinity, was detected at $\phi$ = 0.6, with no significant differences due to the particle surface modification, similarly to what observed in previous work [17].
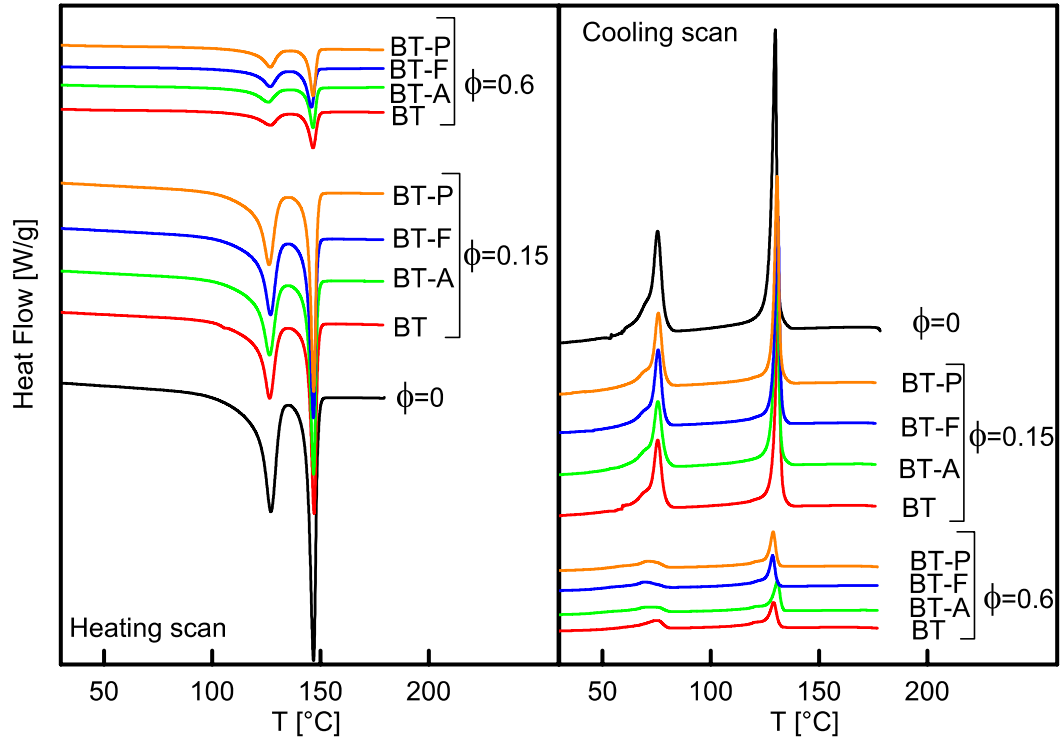


**Fig. 4.** DSC heating and cooling scans of films of P(VDF-TrFE) unfilled ($\phi$ = 0) and filled with BaTiO$_3$ particles, pristine and surface modified ($\phi$ = 0.15 and 0.6).
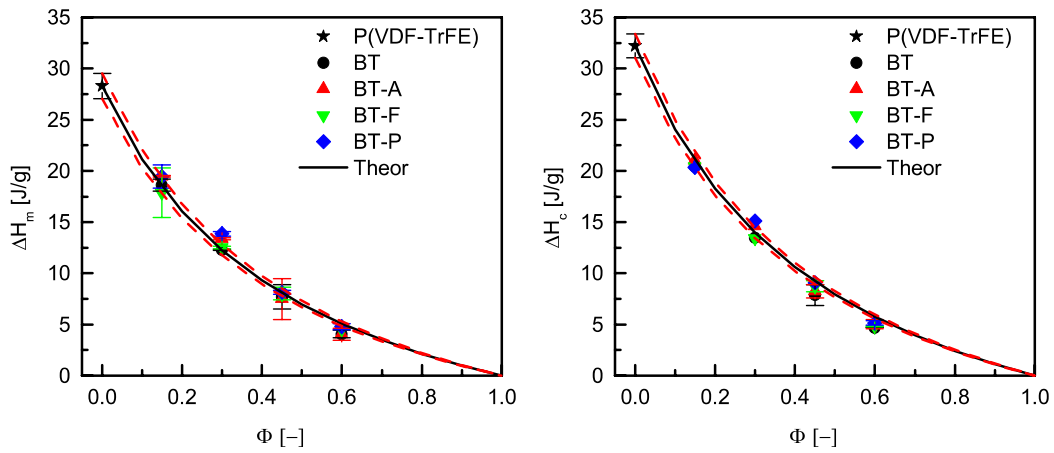


**Fig. 5.** Enthalpy of fusion ($\Delta H_m$) and enthalpy of crystallization ($\Delta H_c$) of film samples as a function of BaTiO$_3$ volume fraction ($\phi$).  The star symbol indicates the unfilled polymer film, the other symbols the composite films containing untreated (BT) and silylated (BT-A, BT-F and BT-P) particles. The solid line indicates the theoretical $\Delta H$ at each BaTiO$_3$ content, calculated from

the ΔH of the pure polymer film, and the dashed lines give the error on the theoretical

calculation due to the error on the measured ΔH of the pure polymer.


The X-ray diffraction pattern of P(VDF-TrFE) films showed a peak at $2\theta = 20°$ attributed to the

ferroelectric β-phase of the polymer (Fig. 6A). The peaks characteristic of α-phase were not

detected. The β-phase peak was also investigated for the films with $\phi = 0.15$ and appeared with

the same shape and position as for the pure polymer, showing that the inclusion of $BaTiO_3$,

pristine or silylated, did not significantly alter the crystalline form of the polymer at this

concentration (Fig. 6A). The XRD scans taken in the $2\theta = 44.5° - 46°$ region on films with $\phi =$

0.6 (Fig. 6B) are unchanged with respect to those of the pristine $BaTiO_3$ in powder form. The

ratio of the intensities of (002) and (200) reflections is approximately 1:2, indicating equal

distribution of ferroelectric domains with polarization in the plane of the film and perpendicular to

the film surface. This indicates that the domain structure of $BaTiO_3$ within the composite is not

affected either by the surface modification or by the film fabrication process. On the other hand,

XRD scans of the same region in composite films with $\phi = 0.15$ (Fig. 6C) showed reduced

intensity of the (002) plane reflection with respect to the powder scan, with no significant

difference due to the type of particle. This indicates a lower fraction of domains with polarization

perpendicular to the film plane, which could be consequence of stresses or texturing in the

composite with the higher amount of matrix surrounding the particles. The apparent shifts in the

peaks' positions are instead most probably due to slight mispositioning of the films in the
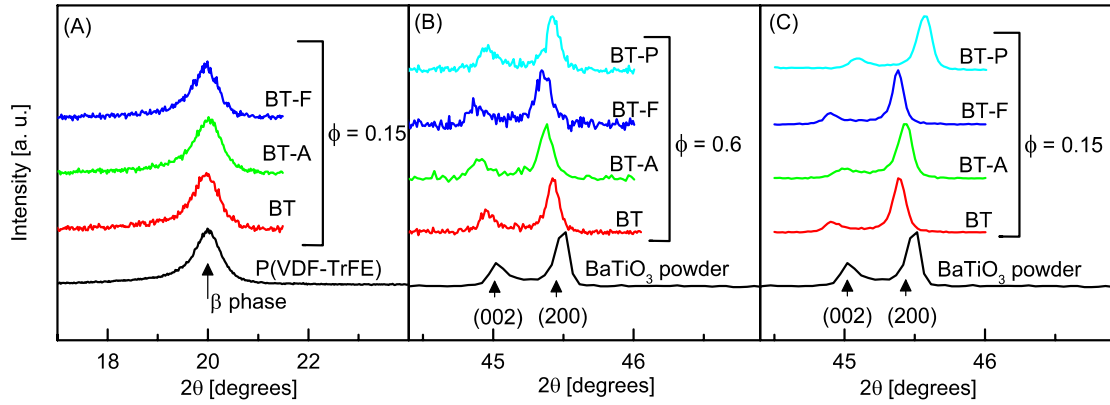
sample holder.

**Fig. 6.** X-ray diffraction patterns of (A) unfilled P(VDF-TrFE) and composites with $\phi = 0.15$ showing the reflection peak corresponding to the polymer's crystalline β-phase, and (B and C) composites with $\phi = 0.6$ and $\phi = 0.15$ showing the reflection peaks of the (002) and (200) planes of $BaTiO_3$.

## 3.3. Thermomechanical properties

Figures 7 and 8 show the results of the dynamic mechanical analysis. For the composites with $\phi = 0.3$ and $\phi = 0.45$ of BT-P it was not possible to obtain proper specimens for testing as they consistently broke while cutting them. In Fig. 7 are reported the experimental E' values at 25 °C and the upper and lower bounds calculated with the Hashin-Shtrickman (HS) model [29] as a function of $\phi$.
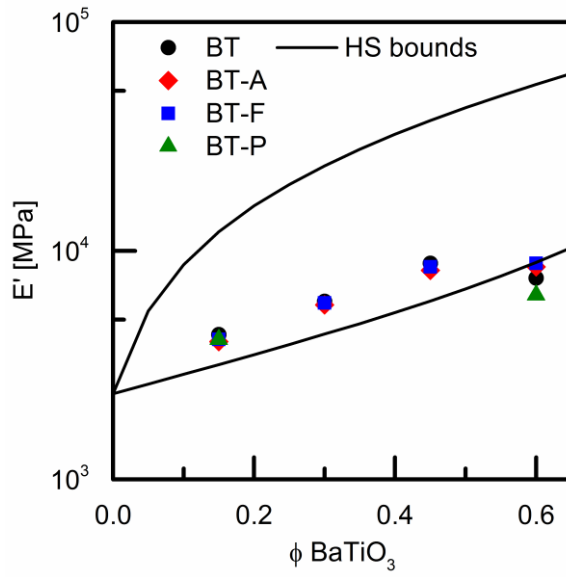
**Fig. 7.** Storage modulus (E') of the composites at 25 °C and upper and lower bounds calculated with the Hashin and Shtrickman model (HS) as a function of $BaTiO_3$ volume fraction.

With pristine particles, E' increased with $\phi$ up to a value of 8.8 GPa at $\phi = 0.45$, then slightly decreased to 7.6 GPa for $\phi = 0.6$, a value not far from the HS lower bound of 8.9 GPa. In previous work, where similar $BaTiO_3$ particles as in this work were used, a value of only about 3.2 GPa, well below the HS lower bound, was obtained with $\phi = 0.6$ of untreated particles, due to poor dispersion and high porosity [17]. No other dynamic mechanical analysis data for solvent cast composites with pristine $BaTiO_3$ particles up to this high concentration were found for comparison. The E' obtained with BT-A and BT-F particles were similar as with pristine particles up to $\phi = 0.45$, and still slightly increased at $\phi = 0.6$, to 8.5 GPa and 8.8 GPa, respectively. The modulus obtained with BT-A particles, as expected, was similar to that found in our previous work for similar composites, i.e. 8.2 GPa, as the aminosilane treatment facilitated good particle dispersion with all mixing conditions [17]. The composites with $\phi = 0.6$ of BT-P had much lower modulus than with all the other types of particles.
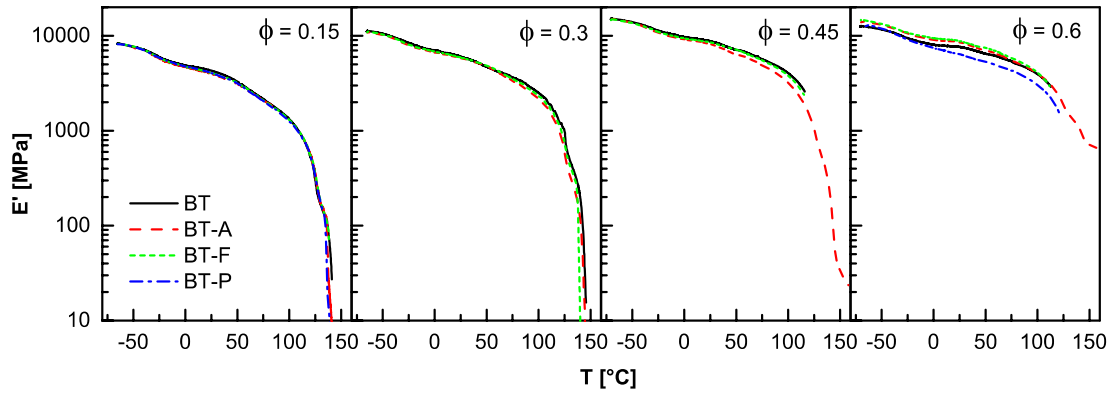
**Fig. 8.** Storage modulus (E') as a function of temperature for composites containing pristine and modified particles.

The storage moduli, E', of the different composites as a function of temperature are reported in Fig. 8, and the corresponding tan$\delta$ curves are reported in Figure S2 of the Supplementary Information. The storage moduli E' of composites with $\phi$ = 0.15 and $\phi$ = 0.3 did not show major differences attributable to the surface modification of the filler in the entire temperature range. For the composites with $\phi$ = 0.45, the storage moduli were comparable for BT, BT-A and BT-F at low temperature; when temperature increased the composites containing BT-A showed a somewhat faster decrease of E' than the others but always resisted until the melting temperature of the matrix (about 150 °C), while more than half of the tested specimens containing pristine BT particles and all the tested specimens containing BT-F broke at about 110 °C under the small strain applied during the DMA test. Similarly, for $\phi$ = 0.6 only the composites filled with BT-A particles did not fail until the melting temperature of the matrix, while for all the other types of particles all the tested specimens failed around 100 °C. In order to understand this effect, the average distance $h$ between two neighbor filler particles can be considered [30]:

$$\frac{h}{d} = \left[ \left( \frac{1}{3\pi\phi} + \frac{5}{6} \right)^{\frac{1}{2}} - 1 \right] \qquad (1)$$

16

With a particle diameter $d$ = 200 nm, assuming monodispersed particles, for $\phi$ = 0.6, $h$ is as low as 1.01 nm (for $\phi$ = 0.15, $h$ = 48.3 nm; for $\phi$ = 0.3, $h$ = 17.9 nm; for $\phi$ = 0.45, $h$ = 6.80 nm); at such high concentration, close to the random packing limit of $\phi$ = 0.64, all polymer chains are in contact with the surface of the particles, treated or not, i.e., interfacial interactions dominate effects such as fracture toughness. In the case of highly filled composites, the BT-A composites, despite having at $\phi$ = 0.6 slightly higher porosity, and hence slightly lower E', than BT-F composites, show better thermomechanical stability. This suggests that, among the silylated particles, only those modified with APTES formed a stronger interface with the polymer, possibly due to the combined effect of a lower surface energy compared to the pristine particles and to the possibility of H-bond formation between the amine group of the silane and the F atoms of the polymer, as proposed by some authors [31,32]. In contrast, TFPTMS and PTMS did not allow for the formation of strong matrix-particle bonds, as also highlighted by SEM observation.

*3.4. Dielectric properties*

The relative permittivity ($\varepsilon_r$) and dielectric loss tangent (tan$\delta_{diel}$) of the P(VDF-TrFE) and composite films, reproduced in Fig. 9, showed the typical features observed for this polymer [33]. For neat P(VDF-TrFE) relative permittivity had a nearly constant value, $\varepsilon_r$ = 10, at frequencies lower than $10^4$ Hz, and decreased at higher frequencies. The tan$\delta_{diel}$ had a value lower than 0.02 below $2\times10^3$ Hz and increased at higher frequencies; the peak that appears at frequencies above $10^6$ Hz is related to the $\alpha_a$ relaxation process, associated with the glass transition of PVDF-TrFE. According to some authors this relaxation originates from the micro-Brownian cooperative movement of the amorphous phase chain segments, while others attribute it to movements of the crystalline-amorphous interphase [1,34–36]. The $\varepsilon_r$ of sintered pristine BaTiO$_3$ was measured to be around 2100 in the entire range of frequencies, with tan$\delta_{diel}$ < 0.02. For the composites, $\varepsilon_r$ was generally lower with surface modified particles than with pristine particles, following the order BT-P<BT-A<BT-F<BT; the differences between the $\varepsilon_r$ values due to surface modification were larger at the higher particle volume fractions. All the

composites with $\phi = 0.15$ had fairly constant $\varepsilon_r$ and tan $\delta_{diel}$ values in the low frequency range, while the composites with $\phi \geq 0.3$ containing pristine $BaTiO_3$ showed a stronger frequency dependence of the dielectric properties at frequencies below $10^4$ Hz than their homologues made with treated particles. Since the effect is present in the samples with the same concentration of $BaTiO_3$ particles it is reasonable to ascribe it to interfacial effects, which are expected to be different for particles treated with silanes with different functional groups.  The presence of the silane layer may indeed modify the charge distribution at the polymer-ceramic interface [37], modifying the interfacial effects. The most effective suppression of interfacial effects was obtained with APTES modified particles, leading to tan$\delta_{diel} \leq 0.02$ in the $10^2$ - $10^4$ Hz range, comparable to that of the unfilled polymer, even for composites with $\phi = 0.6$.  Similar effects were previously attributed to Maxell-Wagner-Sillars (MWS) interfacial polarization [38] which was found to be strong in composites with small (< 500 nm) untreated particles [39].
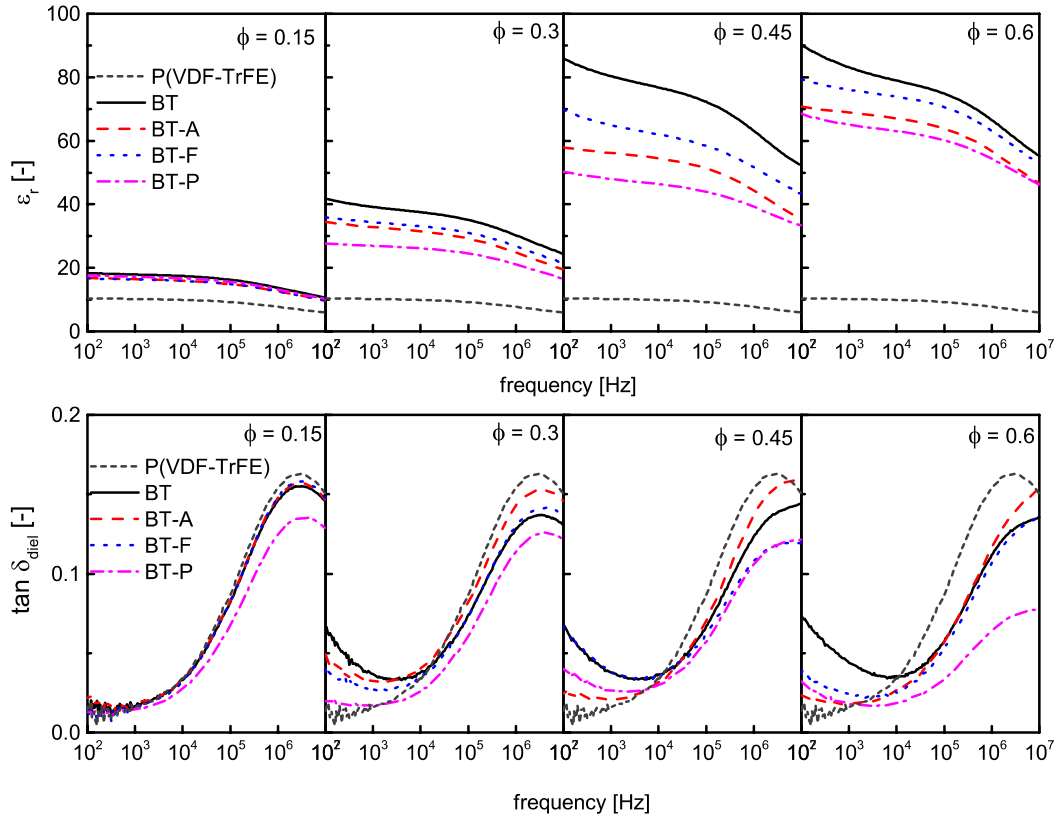
**Fig. 9.** Relative permittivity ($\varepsilon_r$) and dielectric losses ($\tan\delta_{diel}$) as a function of frequency of composites containing pristine and modified particles. As a reference, plots for unfilled P(VDF-TrFE) are reported in all graphs (grey short dash line).

The evolution of the values of $\varepsilon_r$, measured at $10^4$ Hz and at $10^7$ Hz, with the volume fraction $\phi$ of BaTiO$_3$ particles is shown in Fig. 10 (full symbols), together with the permittivity values predicted by two models, proposed by Bruggeman and by Jayasundere et al. [40,41]. Note that these models (as well as others available in the literature) do not include effects of dispersion and geometrical details. A description of the application of these models to P(VDF-TrFE)/BaTiO$_3$ composites can be found elsewhere [6]. The values used in this work for the relative permittivities of P(VDF-TrFE) and of the BaTiO$_3$ particles were the measured values at the respective frequencies, i.e. 10.4, 10.0 and 5.8 for the polymer and 2130, 2100 and 2164 for the particles.



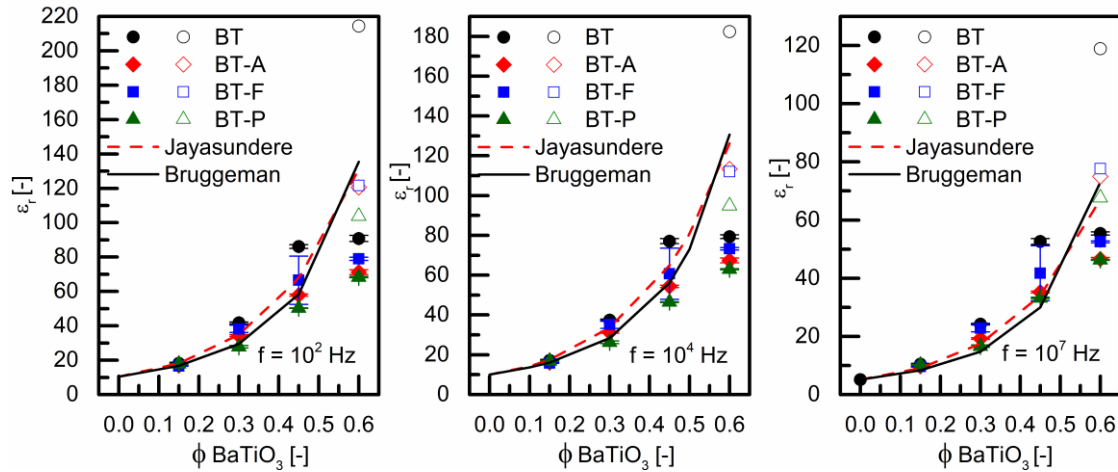**Fig. 10.** Relative permittivity (at $10^2$ Hz, $10^4$ Hz and $10^7$ Hz) as a function of BaTiO$_3$ volume fraction ($\phi$) of composites containing pristine and modified particles (full symbols indicate the measured permittivity and hollow symbols indicate the permittivity of the non-porous composite calculated with eq. 3), and predictions obtained with the Bruggeman and the Jayasundere models.

For the composites with $\phi \leq 0.3$ of both pristine and modified particles, as well as with $\phi = 0.45$ of silylated particles, the values of $\varepsilon_r$ were well in line with the predictions of the models. Furthermore, although a comparison with literature data must take into account that the permittivity of the BaTiO$_3$ particles, and hence of the composites, depends on several factors, including e.g. grain size, impurities and defect concentration, the permittivity values obtained here are comparable to those reported in literature [14,42–46] . Remarkably, the $\varepsilon_r$ value close to 80, obtained here with $\phi = 0.45$ of BT, was not only higher than those reported for similar solvent cast composites with pristine BaTiO$_3$ particles, which were generally below 60 [7,45,47], but also sensibly higher than both the values obtained here with all silylated particles and the values predicted by the models. Finally, above this volume fraction the relative permittivity still increased with $\phi$ with all particles, although to a lower extent than predicted by the models. The $\varepsilon_r$ values obtained with $\phi = 0.6$ of silylated particles were, as expected, close to the value obtained with aminosilane treated BaTiO$_3$ in our previous work; however, while previously we had found that composites with pristine particles had similar $\varepsilon_r$ as with silylated particles, despite having a much higher porosity, in this work the composites with pristine particles showed higher $\varepsilon_r$ than with silylated ones [17]. No further comparison with other authors' data was possible, as although increasing permittivity up to $\phi = 0.67$ was recently reported for spin coated films containing BaTiO$_3$ particles modified with a fluorosilane, the $\varepsilon_r$ achieved was lower than here possibly because the particles had a very different size [14], and no data were found for solvent cast composites with $\phi = 0.6$ of pristine BaTiO$_3$ particles.

Considering the possible causes of the mismatch between the predicted and experimental values of $\varepsilon_r$ at $\phi = 0.6$, a possible overestimation of the permittivity of the particles, leading to a larger error on the predicted permittivity value at high than at low particle volume fraction, was considered here as unlikely (see Supplementary Information).  A more likely explanation is that the porosity of the films with $\phi = 0.6$, although not large, had a noticeable effect on the permittivity of the composites. This can be taken into account applying the logarithmic rule of mixtures:

$$\log \varepsilon = (1 - \phi_v) \log \varepsilon_{npc} + \phi_v \log \varepsilon_v \qquad (2)$$

where $\varepsilon$, $\varepsilon_{npc}$ and $\varepsilon_v$ are the relative permittivities of the porous composite, of the non-porous composite and of the voids, respectively, and $\phi_v$ is the volume fraction of the voids. The theoretical permittivity $\varepsilon_{npc}$ of a composite without porosity would therefore be:

$$\log \varepsilon_{npc} = (\log \varepsilon - \phi_v \log \varepsilon_v)/(1 - \phi_v) \qquad (3)$$

Indeed, as shown in Fig. 10 (hollow symbols), for composites with silylated particles, the $\varepsilon_{npc}$ calculated from eq. 3 was close to the models' predictions, while the calculated $\varepsilon_{npc}$ for the composites with $\phi = 0.6$ of BT particles was found to be even higher than predicted by the models.

To summarize, two main observations may be reported. The first one is that the permittivities of composites with pristine particles were higher than those of composites with silylated particles. With respect to this,  in several studies the use of silanes to obtain better particle dispersion and decrease porosity in solvent cast PVDF and PVDF-TrFE composites with high particle volume fractions led to increased $\varepsilon_r$, although the opposite effect, i.e. a lower $\varepsilon_r$ with modified particles, was observed for ball-milled or compression molded composites [17,19]. As in the latter case, the higher permittivity obtained here with pristine particles was believed to be the result of two opposite effects: the porosity increase with pristine *versus* silylated particles (that would lead to lower $\varepsilon_r$ ) was in this case relatively small, and a decrease of the permittivity of the surface treated particles, due to the presence of the silane layer, as reported by Beier et al. for n-hexylphosphonic acid modified $BaTiO_3$ particles [48], may have become the predominant effect. The second observation is that the $\varepsilon_r$ of the BT composites with $\phi = 0.45$, and the calculated $\varepsilon_{npc}$ for the BT composites with $\phi = 0.6$, were higher than the $\varepsilon_r$ predicted with the Bruggeman and Jayasundere models. In this case, although a contribution of interfacial polarization to the $\varepsilon_r$ of these composites may be considered at low frequencies, the presence of the effect at frequencies higher than $10^4$ Hz in our experiments may suggest a different

mechanism. One possibility, percolation effects due to the high volume fraction of particles, which could be diminished by the presence of the silane layer, would require further investigation.

## 4. Conclusions

In this work, solvent cast composites with volume fractions as high as 0.6 of $BaTiO_3$ particles, pristine and silylated, were prepared with a procedure that allowed obtaining good dispersion and low porosity with all types of particles. Having obtained materials with similar morphology and structure, we could assume that the observed effects were purely due to the surface chemistry of the particles. Pristine particles, and particles modified with three different silanes, with $CH_3$, $CH_2NH_2$ and $CF_3$ functional groups, were considered. Composites with well dispersed pristine particles had higher permittivity and comparable storage modulus than composites with silylated particles, up to high particle volume fractions. However, they also had the highest dielectric losses at low frequencies, and with high particle volume fractions they did not survive above 100 °C under the small deformation applied in the dynamic mechanical analysis. Although both the aminosilane and the fluorosilane provided a slight increase of the storage modulus for a filler volume fraction of 0.6, only the aminosilane, whose organic chain contained a functional group capable of forming H-bonds with the polymer, provided composites with better thermomechanical stability, highlighting the importance of creating stronger interfacial bonds *versus* a simple surface energy reduction. The aminosilane also decreased dielectric losses at low frequencies, to a higher extent than the silanes that contained alkyl or fluorinated chains. Overall, the use of the silane with an alkyl chain led to composites with worse dielectric and thermomechanical properties. These findings contribute to create a knowledge base for a more rational choice of the surface modification and dispersion strategies to be used for the manufacturing of such composites. A continued effort to further reduce the porosity at high ceramic volume fractions, combined with a proper choice of the chemistry of the particle surface modifier, will allow achieving a good compromise between thermomechanical stability and dielectric properties.

**References**

[1]    R. Gregorio, E.M. Ueno, Effect of crystalline phase, orientation and temperature on the dielectric properties of poly (vinylidene fluoride)(PVDF), J. Mater. Sci.. 34 (1999) 4489–4500.

[2]    F. Oliveira, Y. Leterrier, J.-A. Manson, O. Sereda, A. Neels, A. Dommann, D. Damjanovic, Process Influences on the Structure, Piezoelectric, and Gas-Barrier Properties of PVDF-TrFE Copolymer, J. Polym. Sci. B Polym. Phys. 52 (2014) 496–506. doi:10.1002/polb.23443.

[3]    M.M. Vijatovic, J.D. Bobic, B.D. Stojanovic, History and challenges of barium titanate: Part II, Sci. Sinter. 40 (2008) 235–244. doi:10.2298/SOS0803235V.

[4]    T.M. Shaw, Z. Suo, M. Huang, E. Liniger, R.B. Laibowitz, J.D. Baniecki, The effect of stress on the dielectric properties of barium strontium titanate thin films, Appl. Phys. Lett. 75 (1999) 2129–2131.

[5]    M. Wegener, K. Arlt, PZT/P(VDF-HFP) 0-3 composites as solvent-cast thin films: preparation, structure and piezoelectric properties, J. Phys. D Appl. Phys. 41 (2008) 165409 p1–6. doi:10.1088/0022-3727/41/16/165409.

[6]    S. Dalle Vacche, F. Oliveira, Y. Leterrier, V. Michaud, D. Damjanovic, J.-A.E. Månson, The effect of processing conditions on the morphology, thermomechanical, dielectric, and piezoelectric properties of P(VDF-TrFE)/BaTiO$_3$ composites, J. Mater. Sci. 47 (2012) 4763–4774. doi:10.1007/s10853-012-6362-x.

[7]  Y.J. Niu, K. Yu, Y.Y. Bai, H. Wang, Enhanced Dielectric Performance of $BaTiO_3$/PVDF Composites Prepared by Modified Process for Energy Storage Applications, IEEE Trans. Ultrason. Ferroelectr. Freq. Control. 62 (2015) 108–115. doi:10.1109/tuffc.2014.006666.

[8]  Y.P. Mao, S.Y. Mao, Z.G. Ye, Z.X. Xie, L.S. Zheng, Size-dependences of the dielectric and ferroelectric properties of $BaTiO_3$/polyvinylidene fluoride nanocomposites, J. Appl. Phys. 108 (2010) 014102 p 1–6. doi:10.1063/1.3443582.

[9]  J. Fu, Y. Hou, Q. Wei, M. Zheng, M. Zhu, H. Yan, Advanced $FeTiNbO_6$/poly(vinylidene fluoride) composites with a high dielectric permittivity near the percolation threshold, J. Appl. Phys. 118 (2015) 235502 p 1–6. doi:10.1063/1.4937581.

[10] B. Natarajan, Y. Li, H. Deng, L.C. Brinson, L.S. Schadler, Effect of Interfacial Energetics on Dispersion and Glass Transition Temperature in Polymer Nanocomposites, Macromolecules. 46 (2013) 2833–2841. doi:10.1021/ma302281b.

[11] Y. Li, T.M. Krentz, L. Wang, B.C. Benicewicz, L.S. Schadler, Ligand Engineering of Polymer Nanocomposites: From the Simple to the Complex, ACS Appl. Mater. Interfaces. 6 (2014) 6005–6021. doi:10.1021/am405332a.

[12] Y. Huang, T.M. Krentz, J.K. Nelson, L.S. Schadler, M. Bell, B. Benicewicz, Bimodal Brush Functionalized $TiO_2$/silicone Nanocomposites with Improved Dielectric Properties, 2015 IEEE Electrical Insulation Conference (EIC). (2015) 325–328.

[13] P.K. Mahato, S. Sen, Effect of surface modification of ceramic particles by SDS on the electrical properties of PZT-PVDF and BT-PVDF composites: interface effect, J. Mater. Sci. Mater. Electron. 26 (2015) 2969–2976.

[14] N. Kamezawa, D. Nagao, H. Ishii, M. Konno, Transparent, highly dielectric poly(vinylidene fluoride) nanocomposite film homogeneously incorporating $BaTiO_3$ nanoparticles with fluoroalkylsilane surface modifier, Eur. Polym. J. 66 (2015) 528–532. doi:10.1016/j.eurpolymj.2015.03.021.

[15] S. Liu, S. Xue, W. Zhang, J. Zhai, Enhanced dielectric and energy storage density induced by surface-modified $BaTiO_3$ nanofibers in poly(vinylidene fluoride) nanocomposites, Ceram. Int. 40 (2014) 15633–15640. doi:10.1016/j.ceramint.2014.07.083.

[16] X. Zhang, Y. Ma, C. Zhao, W. Yang, High dielectric constant and low dielectric loss hybrid nanocomposites fabricated with ferroelectric polymer matrix and BaTiO$_3$ nanofibers modified with perfluoroalkylsilane, Appl. Surf. Sci. 305 (2014) 531–538. doi:10.1016/j.apsusc.2014.03.131.

[17] S.Dalle Vacche, F. Oliveira, Y. Leterrier, V. Michaud, D. Damjanovic, J.-A.E. Månson, Effect of silane coupling agent on the morphology, structure, and properties of poly(vinylidene fluoride–trifluoroethylene)/BaTiO$_3$ composites, J. Mater. Sci. 49 (2014) 4552–4564. doi:10.1007/s10853-014-8155-x.

[18] K.A. Iyer, J.M. Torkelson, Importance of superior dispersion versus filler surface modification in producing robust polymer nanocomposites: The example of polypropylene/nanosilica hybrids, Polymer. 68 (2015) 147–157. doi:10.1016/j.polymer.2015.05.015.

[19] Y. Niu, K. Yu, Y. Bai, F. Xiang, H. Wang, Fluorocarboxylic acid-modified barium titanate/poly(vinylidene fluoride) composite with significantly enhanced breakdown strength and high energy density, RSC Adv. 5 (2015) 64596–64603. doi:10.1039/C5RA09023G.

[20] X. Huang, L. Xie, K. Yang, C. Wu, P. Jiang, S. Li, S. Wu, K. Tatsumi, T. Tanaka, Role of Interface in Highly Filled Epoxy/BaTiO$_3$ Nanocomposites. Part II-Effect of Nanoparticle Surface Chemistry on Processing, Thermal Expansion, Energy Storage and Breakdown Strength of the Nanocomposites, IEEE Trans. Dielectr. Electr. Insul. 21 (2014) 480–487. doi:10.1109/tdei.2013.004166.

[21] J. Su, J. Zhang, Comparison of rheological, mechanical, electrical properties of HDPE filled with BaTiO$_3$ with different polar surface tension, Appl. Surf. Sci. 388 (2016) 531–538. doi:10.1016/j.apsusc.2015.10.156.

[22] R.G. Acres, A.V. Ellis, J. Alvino, C.E. Lenahan, D.A. Khodakov, G.F. Metha, G.G. Andersson, Molecular Structure of 3-Aminopropyltriethoxysilane Layers Formed on Silanol-Terminated Silicon Surfaces, J. Phys. Chem. C. 116 (2012) 6289–6297. doi:10.1021/jp212056s.

[23] M. Crespin, W.K. Hall, The surface chemistry of some perovskite oxides, J. Catal. 69 (1981) 359–370. doi:10.1016/0021-9517(81)90171-8.

[24] R. Simoes, M. Rodriguez-Perez, J. De Saja, C. Constantino, Tailoring the structural properties of PVDF and P(VDF-TrFE) by using natural polymers as additives, Polym. Eng. Sci. 49 (2009) 2150–2157. doi:10.1002/pen.21455.

[25] Y.L. Pan, B. Arkles, J. Kendenburg, Preparation of Aromatic Silanes as High Thermal Stability Coupling Agents, Adv. Mater. Res. 690–693 (2013) 1483–1489. doi:10.4028/www.scientific.net/AMR.690-693.1483.

[26] A.J. Lovinger, T. Furukawa, G.T. Davis, M.G. Broadhurst, Crystallographic changes characterizing the Curie transition in three ferroelectric copolymers of vinylidene fluoride and trifluoroethylene: 1. As-crystallized samples, Polymer. 24 (1983) 1225–1232.

[27] G. Teyssedre, A. Bernes, C. Lacabanne, Cooperative movements associated with the Curie transition in P(VDF-TrFE) copolymers, J. Polym. Sci. B Polym. Phys. 33 (n.d.) 879–890. doi:10.1002/polb.1995.090330603.

[28] F.J. Baltà Calleja, A.G. Gonzàlez Arche, T.A. Ezquerra, C. Santa Cruz, F. Batallán, B. Frick, E.López Cabarcos, Structure and properties of ferroelectric copolymers of poly(vinylidene fluoride), in: H.-G. Zachmann (Ed.), Structure in Polymers with Special Properties, Springer Berlin Heidelberg, 1993: pp. 1–48. doi:10.1007/3-540-56579-5_1.

[29] Z. Hashin, S. Shtrikman, A variational approach to the theory of the elastic behaviour of multiphase materials, J. Mech. Phys. Solids. 11 (1963) 127–140.

[30] L.V. Woodcock, Developments in the non-newtonian rheology of glass forming systems, in: Molecular Dynamics and Relaxation Phenomena in Glasses, Springer, Berlin, Heidelberg, 1987: pp. 113–124. doi:10.1007/3-540-17801-5_7.

[31] Y. Fan, G. Wang, X. Huang, J. Bu, X. Sun, P. Jiang, Molecular structures of (3-aminopropyl)trialkoxysilane on hydroxylated barium titanate nanoparticle surfaces induced by different solvents and their effect on electrical properties of barium titanate based polymer nanocomposites, Appl. Surf. Sci. 364 (2016) 798–807. doi:10.1016/j.apsusc.2015.12.228.

[32] V.K. Tiwari, R.V. Ghorpade, K.L. Kim, G. Song, T. Kim, H. Han, C. Park, Thin and surface adhesive ferroelectric poly(vinylidene fluoride) films with β phase-inducing amino modified porous silica nanofillers, J. Polym. Sci. B Polym. Phys. 54 (2016) 2401–2411. doi:10.1002/polb.24145.

[33] S.H. Zhang, R.J. Klein, K.L. Ren, B.J. Chu, X. Zhang, J. Runt, Q.M. Zhang, Normal ferroelectric to ferroelectric relaxor conversion in fluorinated polymers and the relaxor dynamics, J. Mater. Sci.. 41 (2006) 271–280. doi:10.1007/s10853-006-6081-2.

[34] K. Nakagawa, Y. Ishida, Annealing effects in poly(vinylidene fluoride) as revealed by specific volume measurements, differential scanning calorimetry, and electron microscopy, J. Polym. Sci. Polym. Phys. Ed. 11 (1973) 2153–2171. doi:10.1002/pol.1973.180111107.

[35] C.V. Chanmal, J.P. Jog, Dielectric relaxations in PVDF/BaTiO3 nanocomposites, Express Polym. Lett. 2 (2008) 294–301. doi:10.3144/expresspolymlett.2008.35.

[36] J.W. Sy, J. Mijovic, Reorientational Dynamics of Poly(vinylidene fluoride)/Poly(methyl methacrylate) Blends by Broad-Band Dielectric Relaxation Spectroscopy, Macromolecules. 33 (2000) 933–946. doi:10.1021/ma9907035.

[37] D.L. Ma, T.A. Hugener, R.W. Siegel, A. Christerson, E. Martensson, C. Onneby, L.S. Schadler, Influence of nanoparticle surface modification on the electrical behaviour of polyethylene nanocomposites, Nanotechnology. 16 (2005) 724–731. doi:10.1088/0957-4484/16/6/016.

[38] L.K.H. Vanbeek, The Maxwell-Wagner-Sillars Effect, Describing Apparent Dielectric Loss in Inhomogeneous Media, Physica. 26 (1960) 66–68. doi:10.1016/0031-8914(60)90115-4.

[39] Z.M. Dang, H.P. Xu, H.Y. Wang, Significantly enhanced low-frequency dielectric permittivity in the $BaTiO_3$/poly(vinylidene fluoride) nanocomposite, Appl. Phys. Lett. 90 (2007) 012901 p1–3. doi:10.1063/1.2393150.

[40] D.A.G. Bruggeman, Berechnung verschiedener physikalischer Konstanten von heterogenen Substanzen. I. Dielektrizitätskonstanten und Leitfähigkeiten der Mischkörper aus isotropen Substanzen, Ann. Phys. 24 (1935) 665–679.

[41]  N. Jayasundere, B.V. Smith, Dielectric-Constant For Binary Piezoelectric 0-3 Composites, J. Appl. Phys. 73 (1993) 2462–2466.

[42]  M.N. Almadhoun, U.S. Bhansali, H.N. Alshareef, Nanocomposites of ferroelectric polymers with surface-hydroxylated $BaTiO_3$ nanoparticles for energy storage applications, J. Mater. Chem. 22 (2012) 11196–11200. doi:10.1039/c2jm30542a.

[43]  H.L.W. Chan, M.C. Cheung, C.L. Choy, Study on $BaTiO_3$/P(VDF-TrFE) 0-3 composites, Ferroelectrics. 224 (1999) 541–548.

[44]  M.C. Cheung, H.L.W. Chan, C.L. Choy, Dielectric relaxation in barium titanate/polyvinylidene fluoride-trifluoroethylene composites, Ferroelectrics. 264 (2001) 1721–1726.

[45]  Y. Niu, Y. Bai, K. Yu, Y. Wang, F. Xiang, H. Wang, Effect of the Modifier Structure on the Performance of Barium Titanate/Poly(vinylidene fluoride) Nanocomposites for Energy Storage Applications, ACS Appl. Mater. Interfaces. 7 (2015) 24168–24176. doi:10.1021/acsami.5b07486.

[46]  M.F. Lin, V.K. Thakur, E.J. Tan, P.S. Lee, Surface functionalization of $BaTiO_3$ nanoparticles and improved electrical properties of $BaTiO_3$/polyvinylidene fluoride composite, RSC Adv. 1 (2011) 576–578. doi:10.1039/c1ra00210d.

[47]  R. Gregorio, M. Cestari, F.E. Bernardino, Dielectric behaviour of thin films of β-PVDF/PZT and β-PVDF/$BaTiO_3$ composites, J. Mater. Sci. 31 (1996) 2925–2930. doi:10.1007/BF00356003.

[48]  C.W. Beier, M.A. Cuevas, R.L. Brutchey, Effect of Surface Modification on the Dielectric Properties of $BaTiO_3$ Nanocrystals, Langmuir. 26 (2010) 5067–5071. doi:10.1021/la9035419.